Journal of Heat and Mass Transfer Research

Journal homepage: https://jhmtr.semnan.ac.ir

Semnan University

ISSN: 2383-3068

Research Article

Influences of Gyrotactic Microorganisms and Nonlinear Mixed Bio-Convection on Hybrid Nanofluid Flow over an Inclined Extending Plate with Porous Effects

Arshad Khan [a] *, Muhammad Jawad [b], Farhat Nasir [a], Ishtiaq Ali [c]

[a] *College of Aeronautical Engineering, National University of Sciences and Technology (NUST), Sector H-12, Islamabad, 44000, Pakistan.*

[b] *Center for Numerical Simulation Software in Engineering and Sciences, College of Mechanics and Materials, Hohai University, Nanjing, 211100, PR China.*

[c] *Department of Mathematics and Statistics, College of Science, King Faisal University, Al-Ahsa, 31982, Saudi Arabia.*

ARTICLE INFO

Article history:

Received: 2023-10-08

Revised: 2024-03-30

Accepted: 2024-03-31

Keywords:

Nonlinear mixed convection;
Hybrid nanofluid;
Inclined plate;
Stretching plate;
Gyrotactic microorganisms

ABSTRACT

This study investigates nonlinear mixed convective hybrid nanofluid flow over a spongy, inclined stretching surface. There are numerous applications of nonlinear convection, and it is especially pivotal in predicting weather patterns accurately and optimizing heat transfer for efficient electronic and industrial cooling systems. The flow is also influenced by the porous behavior of the plate and the presence of the microorganisms. The main emphasis is given to analyzing the influence of thermal and mass Grashof numbers for their nonlinear nature upon the flow system. The equations that administered the flow system are converted to dimensionless notations by using suitable variables. The homotopy analysis approach has been used for the solution of modeled equations. It has been perceived in this work that fluid velocity declines with the upsurge in inertial factor, permeability parameter, volume fraction, and magnetic factor. Thermal profiles upsurge with growth in Brownian, thermophoresis factors, Eckert number, and weaken with Prandtl number. Concentration of fluid increases with progression in the thermophoresis factor and drops with greater values of Schmidt number and Brownian factor. Density number has declined with growth in Peclet, bioconvective Lewis numbers, and inclination angle. Over the range $1 \le Nb, Nt, Ec \le 4$ the heat transfer rate jumps from 1.8057 to 2.1332 in case of Nb, from 1.8057 to 2.1968 in case of Nt and it jumps from 1.8057 2.3177 in case of Ec that shows maximum heat transfer rate in case of variations in Eckert number.

Introduction

Mixed convective flows have a widespread spectrum of applications in engineering and industry, such as coolant of electronic equipment, high performance building insulation, nuclear waste repositories, etc. Recently, many studies have been performed to discuss thermal flow properties regarding the influence of mixed convection. Muhammad et al. [1] have discussed the irreversibility production for Darcy-Forchheimer fully developed mixed convective flow past a curved sheet subject to the influence of chemical reactions and revealed that fluid

* **Corresponding author.**
E-mail address: arshad8084@gamil.com

Cite this article as:
Khan, A., Jawad, M., Nasir, F. and Ali, I., 2024. Influences of Gyrotactic Microorganisms and Nonlinear Mixed Bio-Convection on Hybrid Nanofluid Flow over an Inclined Extending Plate with Porous Effects. *Journal of Heat and Mass Transfer Research*, 11(1), pp. 151-166.
https://doi.org/10.22075/JHMTR.2024.23014.1485

velocity has weakened with amplification in Forchheimer number. Waini et al. [2] have inspected the mixed convective flow of a hybrid nanofluid past an expanding and shrinking surface placed vertically upward and have determined two solutions, both for stretching and shrinking cases, with one solution as stable. Safdar et al. [3] inspected mixed convective and thermal radiative MHD Maxwell fluid flow by using the renowned Buongiorno model to control the thermal flow on a permeable stretching surface. Nabwey et al. [4] have discussed mixed convective flow of nanoliquid on a vertically placed porous sheet with the influence of gyrotactic microorganisms and revealed that enhancement in thermophoretic factor has confirmed the growth in skin friction and Sherwood number. Wahid et al. [5] have deliberated on the mixed convective MHD hybrid nanoparticles flow over a porous plate subject to the influence of thermal radiations. Ali et al. [6] discussed mixed convective fluid flow with impacts of Hall and slip constraints.

Recently, the development of the advanced thermal flow of fluids has acquired considerable recognition in industry. One of such fluid is a hybrid nanoliquid, also known as a modified nanofluid, that can be fabricated by mixing two different types of nanoparticles in a base fluid. It has been proved experimentally that such fluids (nanofluid/hybrid nanofluid) have better thermal conductance. Choi and Eastman [7] have familiarized the mixing of nanoparticles in pure fluid. Sharma et al. [8] studied the behavior of fluid with impacts of nanoparticles and duty particles with impacts of thermal radiations. Chu et al. [9] have conducted model based comparison of MHD time-based hybrid nanofluid through a channel subject to the influence of shape of nanoparticles and have exposed that thermal flow has upsurge whereas fluid motion has weakened for expansion in nanoparticles volumetric fraction. Khan et al. [10] have debated on micropolar hybrid nanoparticles flow past a thin moving needle with effect of microorganisms upon the flow system and determined that fluid velocity has depreciated with growth in rotational factor and temperature has upsurge with higher values of nanoparticle volume fraction and material as well as magnetic factors. Eid and Nafe [11] scrutinized the variations in heat conductance and influence of heat generation on MHD hybrid nanoliquid flow through a permeable medium using slip conditions and suction/injection effects upon the fluid flow system. Ojjela [12] has simulated numerically the model for thermal transmission regarding hybrid nanofluid flow and has established that the addition of SiO_2 has augmented further the thermal transmission of fluid. Ali et al. [13] investigated computationally the thermal slip effects on trihybrid nanofluid flow on an elongating sheet with implications of thermal slip effects. Gumber et al. [14] have discussed the motion of hybrid nanoparticles upon a plate subject to the influences of thermal radiations and suction as well as injection upon the flow system. Moreover, Ali et al. [15-18] have used nanofluid to enhance the thermal transportation of pure fluids to maximum level.

The problems involving heat and mass transmissions of different fluid motions upon an inclined surface/plate have attracted the response of many scientists due to their important applications in the areas of astrophysics, geophysics, and many other problems in engineering, such as boundary layer control in aerodynamics and towers cooling, etc. Sabu et al. [19] have studied the impact of nanoparticles on the MHD liquid flow of nanomaterials over a uniform inclined plate and have exposed that temperature has amplified when the angle of inclination has increased by 0.5094%. Kodi and Mopuri [20] have deliberated on time-based MHD fluid flow over an inclined permeable plate with effect of chemically reactive thermal absorption and Soret influences and have established that inclination of plate, magnetic, and Casson factors have retarding the behavior of fluid motion. Osman et al. [21] have considered free convective flow over an inclined surface and have determined the analytical solution by using Laplace transformation to explore the motion, thermal flow, and mass diffusivity behavior of the fluid flow system. Jha and Samaila [22] have inspected the collective influences of thermophoresis and thermal radiations upon buoyancy-driven flow near the permeable inclined plate and have concluded that mass distribution has amplified for expansion in a thermophoretic factor. Sheri et al. [23] deliberated on MHD liquid flow past an inclined plate subject to chemically reactive and thermally radiative effects along with Hall current influence upon the fluid flow. Hazarika et al. [24] studied naturally convective MHD nanoparticle flow on a Darcian regime.

Stretching surfaces play a fundamental role in the thermal flow phenomenon in fluid dynamics. The numerous applications of such flows comprise plastic sheet extrusion, polymer processing, and metallurgy, etc. Ali et al. [25] have scrutinized the magnetic characteristics of nanoparticles upon liquid flow over stretching sheet and discovered that velocity of liquid has declined while thermal motion has expanded with growth in magnetic factor. Sarada et al. [26] have inspected the stimulus of MHD over thermal flow behavior for fluid flow past a stretching sheet and have determined that the development

in thermophoretic factors has decayed the solid and liquid phase for thermal flow rate. Raza-E-Rabi et al. [27] have deliberated computationally on liquid flow over stretching sheets by means of the influence of nanoparticles on fluid. Warke et al. [28] have explored numerically the stagnant point motion of thermally radiative MHD liquid flow on a permeable stretching sheet and have revealed that temperature has augmented while concentration has declined with the upsurge in radiation, magnetic, and chemically reactive factors. Guedri et al. [29] have studied the production of irreversibility and thermal dissipative flow of EMHD trihybrid fluid flow over an elongating surface. Shah et al. [30] have studied bioconvective hybrid nanofluid using chemically reactive microorganism on a stretched sheet. Hazarika et al. [31] investigated the impacts of tri-nanoparticles on behavior of pure fluid flow on an elongated sheet with impacts of MHD and viscous dissipation.

Bio-convection is a famous process in biosciences that is induced by the upward spinning of microorganisms denser than base fluid such as water. Whenever the microorganisms are much denser, then the higher surface of the liquid is normally weakened and leads to creation of bio-convection in the fluid flow system. The presence of microorganisms in fluid affects thermal and mass diffusions. Waqas et al. [32] have debated radiative bioconvective fluid flow over stretched surface subject to Darcy-Forchheimer and slip condition and have revealed that the concentration of microbes has deteriorated with supplementing values of bio-convective Peclet and Lewis numbers. Yusuf et al. [33] inspected the bio-convective MHD fluid flow and production of entropy past an inclined plate with the influence of microorganisms. Khan et al. [34] considered the influence of microorganisms upon micropolar liquid flow past a heated needle using the influence of viscous dissipation and chemically reactive effects. Bhatti et al. [35] scrutinized the MHD liquid flow with microorganism influences past a circular rotary plate induced in an absorbent medium. Das and Ahmed [36] discussed computationally the bio-convective nanofluid flow on an inclined surface. Shah et al. [37] have discussed nonlinear convection hybrid nanofluid on an extending inclined sheet and have used an analytical approach to determine the solution to the modeled problem.

The following points ensured the novelty of current work

- Time free flow has considered upon inclined plate
- Nonlinear mixed convection has considered for proposed model in combination of influence of gyrotactic microorganisms and permeability of plate for the first time in the work of Shah et al. [37]
- Famous Boingiorno model has used in temperature and concentration equations
- Fluid motion has affected by magnetic field

Moreover, the current investigation will answer the following questions:

(i) How do changes in magnetic strength, porosity factor, and Grashof numbers impact velocity?

(ii) What will by the influence of magnetic factor, Prandtl number, Eckert number, thermophoresis and Brownian motion in thermal flow phenomenon?

(iii) How concentration of fluid affects with escalation in Schmidt number thermophoresis and Brownian motion?

(iv) To which extend the density of microorganism is influenced by growth Peclet number, and bio-convective number?

Problem Formulation

Take some fluid with a combination of nanoparticles on an inclined plate surrounded by a permeable medium. The plate is stretching and making an angle Ω with x-axis as depicted in Figure. 1. Further assumptions are stated below:-

- Nonlinear mixed convection has considered for proposed model in combination of influence of gyrotactic microorganisms
- Famous Boingiorno model has used in temperature and concentration equations
- Fluid motion has affected by magnetic field
- The surrounding of fluid motion is presumed to be of Darcy-Forchheimer nature
- T_w, C_w, N_w are temperature, concentration and microorganism concentration at the surface of plate while $T_\infty, C_\infty, N_\infty$ are matching values at free stream

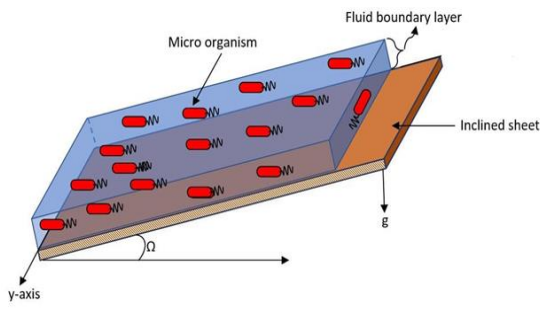

Fig. 1. Flow view in geometrical manner

Using these assumptions we have the following equations [37-39]

$$\frac{\partial v}{\partial y}+\frac{\partial u}{\partial x}=0, \tag{1}$$

$$u\frac{\partial u}{\partial x}+v\frac{\partial u}{\partial y}=\frac{\mu_{hnf}}{\rho_{hnf}}\frac{\partial^2 u}{\partial y^2}+ g\cos\theta\begin{bmatrix}(\rho\beta_T)_{hnf}(T-T_\infty)+(\rho\beta_T)^2_{hnf}(T-T_\infty)^2\\+(\rho\beta_T)_{hnf}(C-C_\infty)+\\(\rho\beta_T)^2_{hnf}(C-C_\infty)^2+(\rho\beta_T)_{hnf}(N-N_\infty)\\+(\rho\beta_T)^2_{hnf}(N-N_\infty)^2\end{bmatrix} -\frac{\sigma_{hnf}}{\rho_{hnf}}\left(B_0^2 u\right)-\frac{\nu_{hnf}}{K}u-\frac{C_b}{\rho_{hnf}\sqrt{K}}u^2, \tag{2}$$

$$u\frac{\partial T}{\partial x}+v\frac{\partial T}{\partial y}=\frac{k_{hnf}}{(\rho c_p)_{hnf}}\frac{\partial^2 T}{\partial y^2}+\frac{\sigma_{nf}B_0^2}{(\rho c_p)_{nf}}u^2 +\frac{(\rho c_p)_p}{(\rho c_p)_{nf}}\left[D_B\left(\frac{\partial C}{\partial y}\frac{\partial T}{\partial y}\right)+\frac{D_T}{T_\infty}\left(\frac{\partial T}{\partial y}\frac{\partial T}{\partial y}\right)\right], \tag{3}$$

$$u\frac{\partial C}{\partial x}+v\frac{\partial C}{\partial y}=D_B\frac{\partial^2 C}{\partial y^2}+\frac{D_T}{T_\infty}\left(\frac{\partial^2 T}{\partial y^2}\right), \tag{4}$$

$$u\frac{\partial N}{\partial x}+v\frac{\partial N}{\partial y}= D_m\frac{\partial^2 N}{\partial y^2}-\frac{b_1 W_e}{(C_w-C_\infty)}\left(\frac{\partial}{\partial y}\left(N\frac{\partial N}{\partial y}\right)\right) \tag{5}$$

The limitations defined at boundaries are

$$\begin{aligned}&u=bx=u_w(x), v=0, T=T_w, N=N_w, C=C_w\\&\quad at\ y=0,\\&u\to 0,\ T\to T_\infty,\ N\to N_\infty,\ C\to C_\infty\\&\quad at\ \ y\to\infty.\end{aligned} \tag{6}$$

in above equations the components of flow along coordinate axes are u,v whereas ρ, D_B, D_T, D_m are density, Brownian, thermophoretic and microorganism diffusions.

The transformation variables are described as:

$$\begin{aligned}&u=bxf'(\eta),\ \eta=y\sqrt{\frac{b}{\nu_f}}, v=-\sqrt{b\nu_f}\,f(\eta),\\&\theta=\frac{T-T_\infty}{T_w-T_\infty},\ \xi=\frac{N-N_\infty}{N_w-N_\infty},\ \Phi=\frac{C-C_\infty}{C_w-C_\infty}.\end{aligned} \tag{7}$$

Using Eq. (7) in Eqs. (1-5) we have

$$\begin{aligned}&\frac{\mu_{hnf}/\mu_f}{2\rho_{hnf}/\rho_f}f'''+\left[\frac{(\beta_T)_{hnf}}{(\beta_T)_f}G_T\theta+\frac{(\beta_T)_{hnf}}{(\beta_T)_f}G_T^*\theta^2\right]\\&+\left[\frac{(\beta_C)_{hnf}}{(\beta_C)_f}G_C\Phi+\frac{(\beta_C)_{hnf}}{(\beta_C)_f}G_C^*\Phi^2\right]\\&+\left[\frac{(\beta_N)_{hnf}}{(\beta_N)_f}G_C\xi+\frac{(\beta_N)_{hnf}}{(\beta_N)_f}G_C^*\xi^2\right]\\&-\frac{\sigma_{hnf}/\sigma_f}{\rho_{hnf}/\rho_f}Mf'-\frac{\nu_{hnf}}{\nu_f}k_1 ff''\\&+f'-\frac{\rho_f}{\rho_{hnf}}F_1 f'-f'^2+ff''=0,\end{aligned} \tag{8}$$

$$\frac{k_{hnf}/k_f}{(\rho c_p)_{hnf}/(\rho c_p)_f}\theta''+\Pr\frac{(\rho c_p)_f}{(\rho c_p)_{hnf}}\left(N_b\Phi'\theta'+N_t\theta'^2\right) +\frac{\sigma_{hnf}/\sigma_f}{(\rho c_p)_{hnf}/(\rho c_p)_f}\Pr MEcf'^2+\Pr f\theta'=0, \tag{9}$$

$$\Phi''+Sc\left(f\Phi'\right)+\frac{N_t}{N_b}\theta''=0, \tag{10}$$

$$\xi''+\Pr L_b\xi' f-P_e\left[\Phi'\xi'+(\xi+\Omega)\Phi''\right]=0 \tag{11}$$

Eq. (6) in dimension less notation is

$$\begin{aligned}&f(0)=0,\ f'(0)=1,\ \theta(0)=1,\xi(0)=1,\Phi(0)=1,\\&f'(\infty)\to 0,\theta(\infty)\to 0,\xi(\infty)\to 0,\Phi(\infty)\to 0 \text{ at } \eta\to\infty.\end{aligned} \tag{12}$$

Where thermophoretic parameter is $N_t=\frac{(\rho c_p)_p D_T(T_w-T_\infty)}{(\rho c_p)_f T_\infty \nu_f}$, Brownian motion parameter is $\mathrm{N}_b=\frac{(\rho c_p)_p D_B(C_w-C_\infty)}{(\rho c_p)_f \nu_f}$, Schmidt number $Sc=\frac{\nu_f}{D_B}$, porosity parameter $k_1=\frac{\mu_f}{\rho_f Kb}$, magnetic field parameter $M=\frac{\sigma\beta_0^2}{\rho_f b}$, $F_1=\frac{C_b x}{\rho_f\sqrt{K}}$ is inertial parameter, $\Pr=\frac{\mu c_p}{k_f}$ is Prandtl number, $Ec=\frac{u_w^2 b}{c_p(T_w-T_\infty)}$ is Eckert number, $P_e=\frac{b_1 W_e}{D_m}$ is Peclet number, $L_b=\frac{\alpha}{D_m}$ is bio-convection Lewis number, $G_T=\frac{\beta_T(T_w-T_\infty)}{b^2 x}g\cos\theta,$, $G_T^*=\frac{(\beta_T)^2(T_w-T_\infty)}{b^2 x}g\cos\theta,$ $G_C=\frac{\beta_C(C_w-C_\infty)}{b^2 x}g\cos\theta,$ $G_C^*=\frac{(\beta_C)^2(C_w-C_\infty)}{b^2 x}g\cos\theta,$ and

$G_N = \frac{\beta_N (N_w - N_\infty)}{b^2 x} g\cos\theta, \quad G_N^* = \frac{\beta_N (N_w - N_\infty)}{b^2 x} g\cos\theta,$
are different Grashof numbers.

1.1. Important Quantities

The quantities of interest are described as follows

$$C_f = \frac{t_w}{\mu_f u_w^2(x)}, \; Nu_x = \frac{x q_w}{k_f (T_w - T_\infty)}, \\ Sh_x = \frac{x q_m}{D_b (C_w - C_\infty)}, \; Nn_x = \frac{x q_m}{D_m (N_w - N_\infty)}, \tag{13}$$

where

$$t_w = -\mu_{hnf}\left(u_y\right)_{y=0}, q_w = -k_{hnf}\left(T_y\right)_{y=0}, \\ q_m = -D_B\left(C_y\right)_{y=0}, q_m = -D_m\left(n_y\right)_{y=0}, \tag{14}$$

By employing Eq. (7) we have from Eq. (13)

$$C_f Re_x^{0.5} = \frac{\mu_{hnf}}{\mu_f} f''(0), NuRe_x^{-0.5} = -\left(\frac{k_{nf}}{k_f}\right)\theta'(0), \\ ShRe_x^{-0.5} = -\Phi'(0), Nn_x \,\mathrm{Re}_x^{-1/2} = -\xi'(0) \tag{15}$$

3. Solution Method

For solution of dimension-free Eqs. (8-11) by employing Eq. (12) the HAM approach [40, 41] has used. The starting values for this method are given by

$$f_0(\eta) = \frac{3}{2\beta^2}(2-S)\left[\frac{\eta^3}{6} - \frac{\beta\eta^2}{2}\right] + \eta, \\ \theta_0(\eta) = 1, \quad \phi_0(\eta) = 1, \quad \xi_0 = 1 \tag{16}$$

The linear operators are given as

$$L_f(f) = A_1\frac{\eta^3}{6} + A_2\frac{\eta^2}{2} + A_3\eta + A_4, \\ L_\theta(\theta) = B_1\eta + B_2, \; L_\phi(\phi) = C_1\eta + C_2, \\ L_\xi(\xi) = D_1\eta + D_2. \tag{17}$$

The non-linear operatives are chosen as $\mathrm{N}_{\hat{f}}, \mathrm{N}_{\hat{\theta}}, \mathrm{N}_{\hat{\Phi}}$ and $\mathrm{N}_{\hat{\xi}}$ and identify in system:

$$\mathrm{N}_{\hat{f}}\left[\hat{f}(\eta;\zeta), \hat{\Theta}(\eta;\zeta), \hat{\Phi}(\eta;\zeta), \hat{\xi}(\eta;\zeta)\right] = \frac{\mu_{hnf}/\mu_f}{2\rho_{hnf}/\rho_f}\hat{f}_{\eta\eta\eta} \\ + \left[\frac{(\beta_T)_{hnf}}{(\beta_T)_f}G_T\hat{\theta} + \frac{(\beta_T)_{hnf}}{(\beta_T)_f}G_T^*\hat{\theta}^2\right] \\ + \left[\frac{(\beta_C)_{hnf}}{(\beta_C)_f}G_C\hat{\Phi} + \frac{(\beta_C)_{hnf}}{(\beta_C)_f}G_C^*\hat{\Phi}^2\right] \\ + \left[\frac{(\beta_N)_{hnf}}{(\beta_N)_f}G_C\hat{\xi} + \frac{(\beta_N)_{hnf}}{(\beta_N)_f}G_C^*\hat{\xi}^2\right] \\ - \frac{\sigma_{hnf}/\sigma_f}{\rho_{hnf}/\rho_f}M\hat{f}_\eta - \frac{\nu_{hnf}}{\nu_f}k_1\hat{f}\hat{f}_{\eta\eta} + \hat{f}_\eta - \frac{\rho_f}{\rho_{hnf}}F_1\hat{f}_\eta - \hat{f}_\eta^2 + \hat{f}\hat{f}_{\eta\eta}, \tag{18}$$

$$\mathrm{N}_{\hat{\theta}}\left[\hat{f}(\eta;\zeta), \hat{\theta}(\eta;\zeta), \hat{\Phi}(\eta;\zeta)\right] = \frac{k_{hnf}/k_f}{\frac{(\rho c_p)_{hnf}}{(\rho c_p)_f}}\hat{\theta}_{\eta\eta} \\ + \Pr\frac{(\rho c_p)_f}{(\rho c_p)_{hnf}}\left(N_t\hat{\Theta}'^2 + N_b\hat{\Phi}'\hat{\Theta}'\right) + \\ \frac{\sigma_{hnf}/\sigma_f}{(\rho c_p)_{hnf}/(\rho c_p)_f}\Pr MEc\hat{f}_\eta^2 + \Pr\hat{f}\hat{\theta}_\eta, \tag{19}$$

$$\mathrm{N}_{\hat{\Phi}}\left[\hat{\Phi}(\eta;\zeta), \hat{f}(\eta;\zeta), \hat{\theta}(\eta;\zeta)\right] = \\ \hat{\Phi}_{\eta\eta} + Sc\hat{f}\hat{\phi}_\eta + \frac{N_t}{N_b}\hat{\theta}_{\eta\eta}, \tag{20}$$

$$\mathrm{N}_{\hat{\xi}}\left[\hat{f}(\eta;\zeta), \hat{\Phi}(\eta;\zeta), \hat{\xi}(\eta;\zeta)\right] = \hat{\xi}_{\eta\eta} \\ + \Pr L_b\hat{\xi}_\eta\hat{f} - P_e\left[\hat{\xi}_\eta\hat{\Phi}_{\eta\eta} + \left(\hat{\xi} + \Omega\right)\hat{\Phi}_{\eta\eta}\right], \tag{21}$$

While BCs are:

$$\left.\frac{\partial\hat{f}(\eta;\zeta)}{\partial\eta}\right|_{\eta=0} = 1, \; \left.\hat{f}(\eta;\zeta)\right|_{\eta=0} = 0, \\ \left.\hat{\theta}(\eta;\zeta)\right|_{\eta=0} = 1, \left.\hat{\Phi}(\eta;\zeta)\right|_{\eta=0} = 1, \\ \left.\hat{\xi}(\eta;\zeta)\right|_{\eta=0} = 1, \\ \left.\frac{\partial\hat{F}(\eta;\zeta)}{\partial\eta}\right|_{\eta=\infty} = 0, \left.\hat{\theta}(\eta;\zeta)\right|_{\eta=\infty} = 0, \\ \left.\hat{\Phi}(\eta;\zeta)\right|_{\eta=\infty} = 0, \left.\hat{\xi}(\eta;\zeta)\right|_{\eta=\infty} = 0, \tag{22}$$

here, ζ is the embedding parameter $\zeta \in [0,1]$, to standardize the convergence of the solution of $\hbar_{\hat{f}}$, $\hbar_{\hat{\theta}}, \hbar_{\hat{\Phi}}$ and $\hbar_{\hat{\xi}}$ is used. By choosing $\zeta = 0$ and $\zeta = 1$ we have:

$$\hat{f}(\eta;1) = \hat{f}(\eta), \hat{\xi}(\eta;1) = \hat{\xi}(\eta), \\ \hat{\theta}(\eta;1) = \hat{\theta}(\eta), \hat{\Phi}(\eta;1) = \hat{\Phi}(\eta), \tag{23}$$

Develop the Taylor's series for $\hat{f}(\eta;\zeta)$, $\hat{\theta}(\eta;\zeta)$, $\hat{\Phi}(\eta;\zeta)$ and $\hat{\xi}(\eta;\zeta)$ about the point $\zeta = 0$

$$\hat{F}(\eta;\zeta) = \hat{F}_0(\eta) + \sum_{n=1}^{\infty}\hat{F}_n(\eta)\zeta^n, \\ \hat{\theta}(\eta;\zeta) = \hat{\theta}_0(\eta) + \sum_{n=1}^{\infty}\hat{\theta}_n(\eta)\zeta^n, \\ \hat{\Phi}(\eta;\zeta) = \hat{\Phi}_0(\eta) + \sum_{n=1}^{\infty}\hat{\Phi}_n(\eta)\zeta^n, \\ \hat{\xi}(\eta;\zeta) = \hat{\xi}_0(\eta) + \sum_{n=1}^{\infty}\hat{\xi}_n(\eta)\zeta^n, \tag{24}$$

$$\hat{f}_n(\eta) = \frac{1}{n!}\left.\frac{\partial\hat{f}(\eta;\zeta)}{\partial\eta}\right|_{p=0}, \; \hat{\theta}_n(\eta) = \frac{1}{n!}\left.\frac{\partial\hat{\theta}(\eta;\zeta)}{\partial\eta}\right|_{p=0}, \\ \hat{\Phi}_n(\eta) = \frac{1}{n!}\left.\frac{\partial\hat{\Phi}(\eta;\zeta)}{\partial\eta}\right|_{p=0}, \hat{\xi}_n(\eta) = \frac{1}{n!}\left.\frac{\partial\hat{\xi}(\eta;\zeta)}{\partial\eta}\right|_{p=0}, \tag{25}$$

4. Results and Discussion

This work is reserved to explore nonlinear mixed convective hybrid nanofluid flow on a porous and inclined stretching surface. The flow is influenced by porous behavior of the plate and the presence of the microorganisms. The main emphasis is given to analyze the influence of thermal and mass Grashof numbers for their nonlinear nature upon flow system. The equations that administered the flow system are converted to dimension-free notations by suitable variables. In the following paragraphs, the impression of various factors upon fluid motion will be discussed.

4.1. Velocity Characteristics

The impression of different physical factors on flow characteristics has been portrayed in Figures. (2-5). An upsurge in the values of inertial factor results a dominancy in the inertial forces due to which maximum constraints is experienced by the fluid particles at the surface of inclined plate. Actually F_1 has a nonlinear relationship against the fluid flow. Moreover, as F_1 enhanced the thickness of fluid particles is enhanced. So with the application of Forchheimer theory the retardation in flow of fluid is visualized. The motion of fluid is retarded gradually for growth in the porosity of inclined surface as F_1 is closely associated with porosity behavior of surface.

Hence fluid motion exhibits retardation for corresponding growth in F_1 as illustrated in Figure 2.

Similarly with greater values of porosity factor k_1 the ability to flow in the absorbent medium is deteriorated as depicted in Figure 3. Physically, when k_1 increases in a porous medium, such as soil or rock, the velocity profiles of fluid flow tend to decline due to heightened porosity and increased resistance to flow within the porous structure. As porosity rises, the available void spaces expand, leading to a more complex and convoluted path for fluid movement. This increased complexity results in a greater resistance to flow, reducing overall flow velocities.

The variations in hybrid nanofluid profiles against different values of magnetic factor M are captured in Figure 4 where a retarding behavior in fluid motion has observed. When M increases in a fluid flow system, the velocity profiles tend to decline due to the emergence of magnetic forces that resist and disrupt the fluid motion. This phenomenon is particularly evident in magnetohydrodynamics (MHD), where a magnetic field interacts with a conducting fluid. The magnetic forces induced in the presence of an intensified magnetic factor act as a damping mechanism, introducing resistance to the fluid flow. This increased resistance manifests as a decline in velocity profiles. Practical applications of this effect can be observed in technologies like magnetic drug targeting, where the controlled manipulation of magnetic nanoparticles in the bloodstream is employed to direct drug delivery to specific targets within the body. Manipulating the magnetic factor in such systems is crucial for optimizing the efficiency and precision of the fluidic processes involved, influencing applications ranging from medical treatments to industrial processes like electromagnetic metal casting.

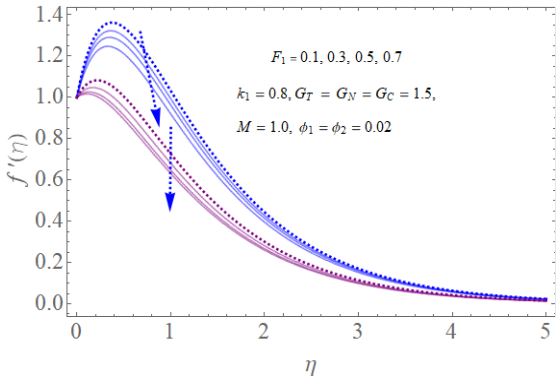

Fig. 2. Flow characteristics Vs variations in inertial parameter

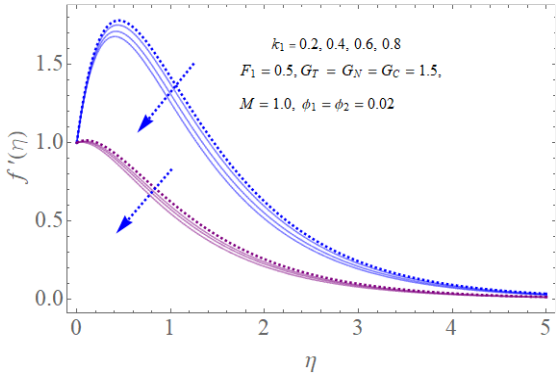

Fig. 3. Flow characteristics Vs variations in permeability parameter.

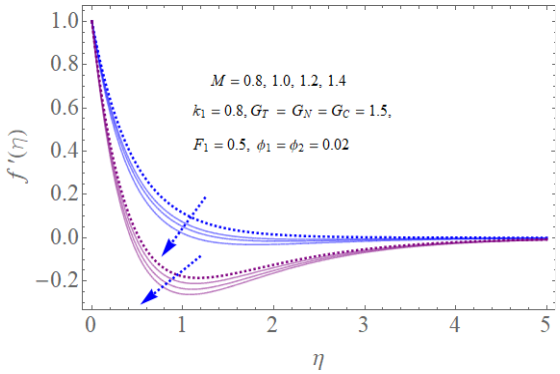

Fig. 4. Flow characteristics Vs variations in magnetic parameter

The variations in fluid motion in response of differences in volume fractions are described in Figure 5. When the volume fraction of nanoparticles increases in a fluid, the velocity profiles typically decline due to heightened viscosity and increased resistance to flow. This phenomenon is particularly pronounced in nanofluids, where nanoparticles are dispersed in a base fluid. As the volume fraction of nanoparticles rises, the effective viscosity of the nanofluid increases, impeding the fluid's ability to flow smoothly. The augmented resistance stems from the interaction between the nanoparticles, causing disruptions in the fluid dynamics.

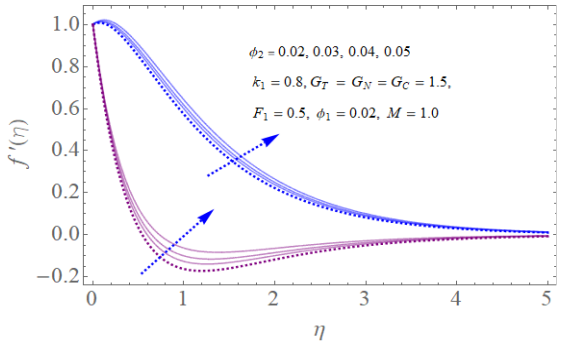

Fig. 5. Flow characteristics Vs variations in nanoparticles volume fraction

4.2. Thermal Characteristics

The effects of different physical factors over temperature have been illustrated in Figures (6-9). It has noticed in Figure 6 that with progression in N_b the haphazard motion with in the fluid upsurge due to more collision amongst the particles. In this way, the kinetic energy of nanoparticles is converted to thermal energy because of which the skin friction augments. Due to the consequence of growth in skin friction, maximum transportation of heat occurs that upsurge the width of thermal layer at the boundaries. Hence with upsurge in N_b the thermal flow augments as depicted in Figure 6, where changes are more significant in case of hybrid nanoparticles.

The conduct of thermal flow in reaction of deviations in thermophoretic factor N_t has illustrated in Figure 7, where an augmenting behavior has noticed in temperature profiles. The process of diffusions of particles under the influence of gradient of temperature is termed as thermophoresis. The potential that results in collecting of nanoparticles due to gradient in temperature at ambient fluid is termed as thermophoresis force. Indeed, when the values of the thermophoresis factor increase, the temperature gradient tends to increase as well. This phenomenon leads to the maximization of the width of the temperature layer at the boundaries. Hence upsurge in N_t causes a progression in thermal profiles as described in Figure 7.

The influences of Prandtl number Pr upon thermal characteristics are depicted in Figure 8 with a declining behavior in heat flow. Physically, when the Prandtl number increases in a fluid, temperature profiles typically decline due to an enhanced thermal diffusivity relative to momentum diffusivity. The Prandtl number is the ratio of momentum diffusivity to thermal diffusivity in a fluid, and a higher Prandtl number signifies that thermal diffusion occurs more rapidly compared to momentum diffusion. This results in a more efficient transfer of heat within the fluid, leading to smoother temperature gradients and a decline in temperature profiles.

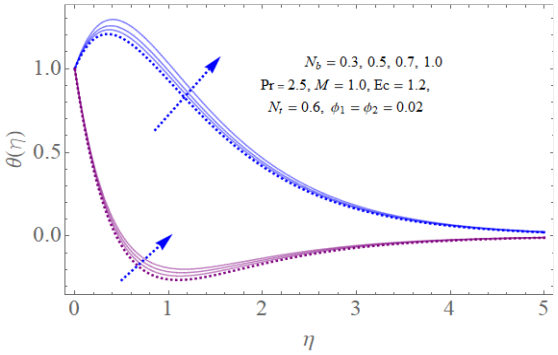

Fig. 6. Thermal characteristics Vs variations in Brownian factor

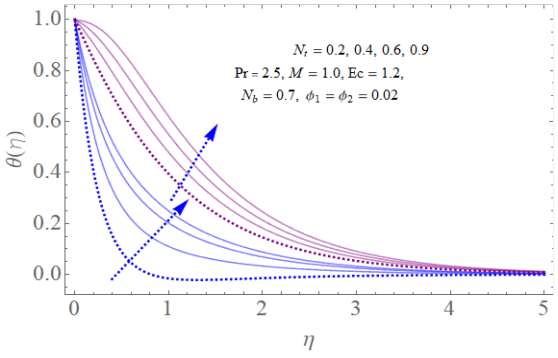

Fig. 7. Thermal characteristics Vs variations in thermophoresis factor

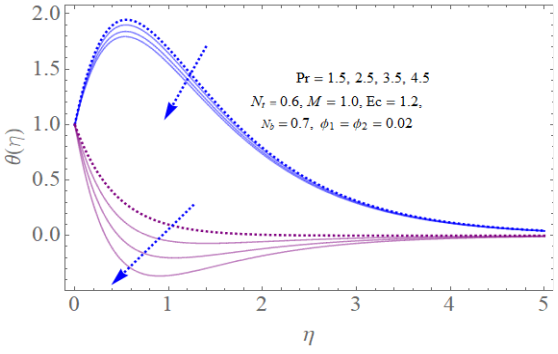

Fig. 8. Thermal characteristics Vs variations in Prandtl number

The performance of temperature in reaction of variations in Eckert number Ec is shown in Figure 9. When the Eckert number increases in a fluid flow system, temperature profiles typically augment due to a higher conversion of kinetic energy into thermal energy. The Eckert number, defined as the ratio of kinetic energy to enthalpy changes, signifies the dominance of kinetic energy in the flow. As the Eckert number rises, a larger portion of the fluid's energy is directed toward increasing temperature rather than kinetic effects. This heightened conversion results in elevated temperature profiles.

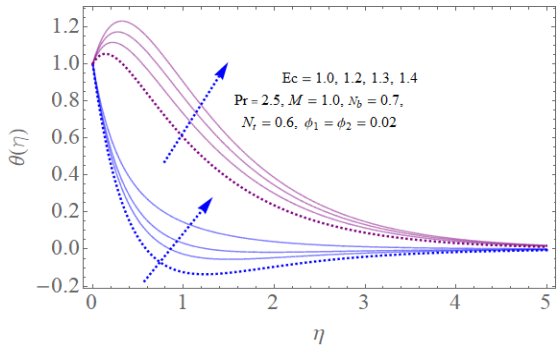

Fig. 9. Thermal characteristics Vs variations in Eckert number

4.3. Concentration Characteristics

The impact of different physical factors on concentration has been described in Figures (10-12). In Figure 10, the impact of Brownian factor N_b upon concentration profiles has depicted with a retarding behavior in concentration. When the Brownian factor increases in a fluid system, concentration profiles typically decline due to heightened random motion and dispersion of particles. Brownian motion is the random movement of particles suspended in a fluid caused by collisions with surrounding molecules. An upsurge in the Brownian factor signifies an increase in this random motion, making it more challenging for particles to maintain a concentrated distribution. The physical reason behind the decline in concentration profiles is that as Brownian motion becomes more pronounced, particles diffuse more extensively throughout the fluid, leading to a more uniform dispersion.

With higher values of thermophoretic factor N_t, the concentration panel augments as illustrated in Figure 11. When the thermophoresis factor increases in a fluid system, concentration profiles typically augment due to enhanced particle migration in response to temperature gradients. Thermophoresis refers to the motion of particles induced by temperature variations in a fluid. An upsurge in the thermophoresis factor indicates a greater sensitivity of particle motion to temperature changes. The physical reason behind the augmentation of concentration profiles is the intensified thermophoretic force acting on particles, causing them to move preferentially toward regions of higher to lower temperature, depending on the characteristics of the particles.

The performance of concentration profiles as a reaction of deviations in Schmidt number Sc is portrayed in Figure 12. It has perceived in this figure that Sc has an opposing impression over the concentration profiles. Actually, with upsurge in Sc the diffusion of mass declines as a consequence of which the concentration retards. Physically, with growth in Sc the particles of fluid at the surface of inclined plate defuse at a minimum level as a result of which lesser mass transportation of fluid occurs. Hence, growth in Sc drops the concentration of fluid as described in Figure 12.

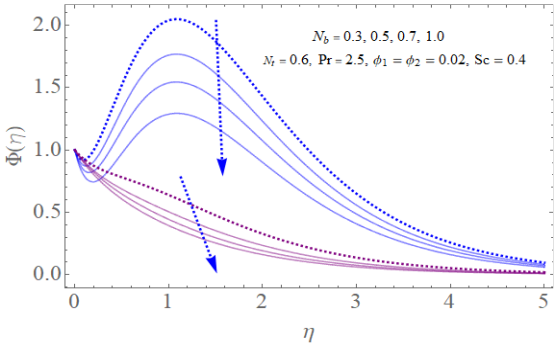

Fig. 10. Concentration characteristics Vs variations in Brownian factor

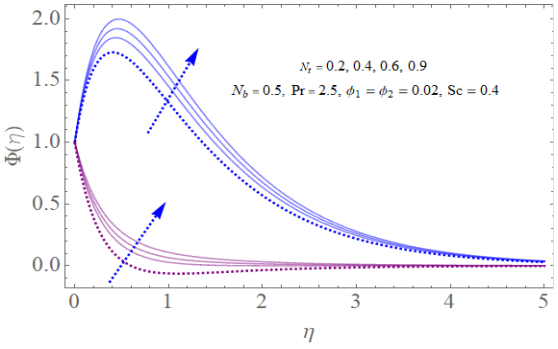

Fig. 11. Concentration characteristics Vs variations in thermophoresis factor

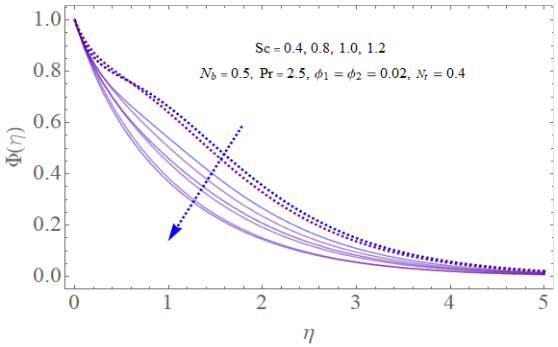

Fig. 12. Concentration characteristics Vs variations in Schmidt number.

4.4. Motile Microorganism Characteristics

The presentation of microorganism profiles due to deviations in various evolving factors has been presented in Figures (13-15). In Figure 13 and 14 we observe that motile density has declined with upsurge in L_b and Peclet number P_e. When both the Bio-convection Lewis number and Peclet number increase in a fluid system, microorganism density profiles typically decline due to enhanced mass transfer and dispersion effects. The Bio-convection Lewis number characterizes the ratio of thermal diffusion to mass diffusion, while the Peclet number represents the ratio of advective transport to diffusive transport. An upsurge in these numbers implies that advection and mass transfer become more dominant relative to diffusion. The physical reason behind the decline in microorganism density profiles is the increased efficiency of fluid flow in transporting and dispersing microorganisms, leading to a more uniform distribution.

Moreover, L_b is inversely proportional to diffusion of microorganism (D_m), so with growth in L_b, less diffusion occurs in microorganism that justifies the decline in $\xi(\eta)$. Similarly in Figure 14 a decline in $\xi(\eta)$ has noticed for growth in Peclet number P_e. Again as P_e is inversely proportional to diffusion of microorganism D_m, and directly proportional to swimming speed of cells (W_c) and chemotaxis constant (b_1), so growth in P_e is again associated with less diffusion of microorganism. As a consequence of this phenomenon the motile density of microorganism decline as illustrated in Figure 14.

Moreover, the escalating values of inclination angle (Ω) also depressed the motile density of microorganism $\xi(\eta)$ as portrayed in Figure 15. Since the flow of fluid is upon the inclined plate so with upsurge in the values of (Ω) less microbes are shifted to the upper surface of the fluid due to which the diffusion of microorganism affected adversely. Therefore with progression in (Ω) the values of $\xi(\eta)$ are diminished gradually as presented in Figure 15.

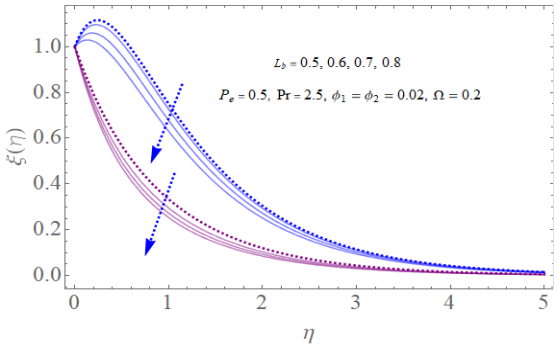

Fig. 13. Microorganism characteristics Vs variations in bioconvection Lewis number

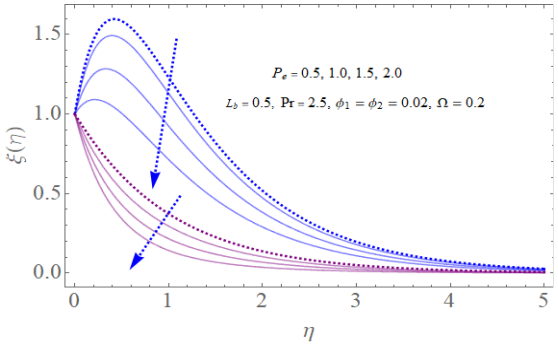

Fig. 14. Microorganism characteristics Vs variations in Peclet number

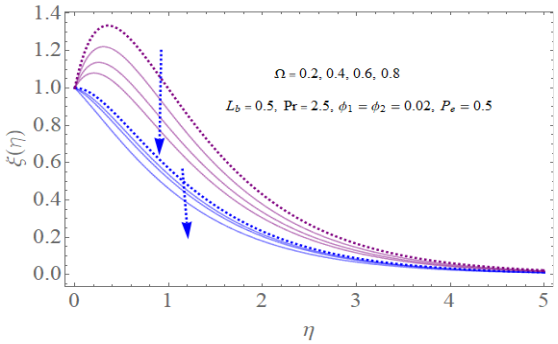

Fig. 15. Microorganism characteristics Vs variations in angle of inclination.

4.5. Heat Transfer Rate

An increase in the Brownian motion factor, thermophoresis factor, and Eckert number collectively leads to an upsurge in heat transfer rates. Higher Brownian motion intensifies the random movement of particles, enhancing their collision frequency and thus augmenting heat transfer in, for example, nanofluid systems. Elevated thermophoresis factors imply enhanced particle migration in response to temperature gradients, contributing to increased convective heat transfer. Additionally, a rising Eckert number indicates a larger proportion of kinetic energy converted into thermal energy, amplifying overall heat transfer.

In practical terms, this enhanced heat transfer can be harnessed in applications such as advanced heat exchangers and nanofluid-based cooling systems, where optimizing Brownian motion, thermophoresis, and kinetic-to-thermal energy conversion are crucial for efficiency improvements and thermal management strategies. It has noticed in Figure. 16 that when Nb move from 1 to 4, the heat transfer rate jumps from 1.8057 to 2.1332, for Nt moving from 1 to 4 the heat transfer rate jumps from 1.8057 to 2.1968. Similarly, for variations in Ec from 1 to 4, the heat transfer rate moves from 1.8057 2.3177. This phenomenon shows maximum heat transfer rate in case of variations in Eckert number.

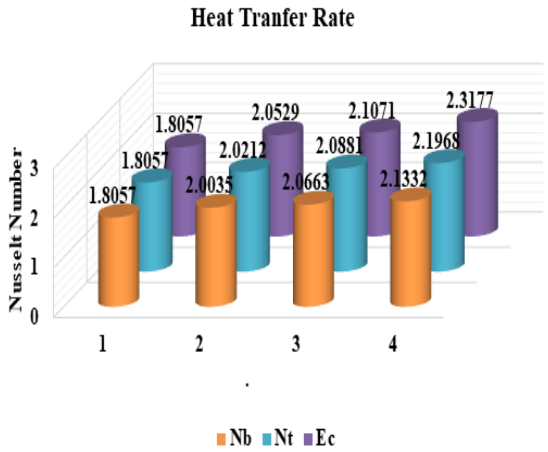

Fig. 16. Heat transfer rate phenomenon for Nb, Nt, Ec

4.6. Tables Discussion

In Table 1, the influence of different merging factors upon skin friction has portrayed numerically. Since the upsurge in the values of inertial factor results dominancy in the inertial forces due to which maximum constraints is experienced by the fluid particles at the surface of inclined plate. The motion of fluid is retarded gradually for growth in the inertial factor due to which skin friction augments. Similarly, growth in volume fraction and magnetic factors retards motion of the fluid and upsurge the skin friction.

Table 2 depicts numerically the impact of different factors upon Nusselt number. Since the temperature distribution augments with upsurge in magnetic factor, volume fraction, thermophoresis and Brownian motion factors, hence these factors affect adversely the Nusselt number.

Growth in thermophoresis factor, and Schmidt number decline the Sherwood number as depicted in Table 3 numerically. Growth in Brownian motion factor, and Prandtl numbers increase the Sherwood number as depicted in Table 3 numerically.

Table. 1. Impact of different physical factors on $C_{fx}Re_x^{0.5} = (\mu_{hnf}/\mu_f) f''(0)$

M	k_1	F_1	ϕ_2	$C_{fx}Re_x^{0.5}$
0.8	0.2	0.1	0.02	3.97807
1.0				3.98144
1.2				3.98486
1.2	0.2	0.1	0.02	3.96849
	0.4			3.97045
	0.6			3.97231
0.8	0.2	0.1	0.02	3.99166
		0.3		3.99498
		0.5		3.99837
0.8	0.2	0.1	0.02	2.23086
			0.03	2.34403
			0.04	2.46735

Table. 2. Impact of different physical factors on $NuRe_x^{-0.5} = -(k_{nf}/k_f)\theta'(0)$

M	N_b	N_t	ϕ_2	Pr	$NuRe_x^{-0.5}$
0.8	0.3	0.2	0.01	1.5	1.09554
1.0					1.09214
1.2					1.08876
0.8	0.3	0.2	0.01	1.5	1.07696
	0.5				1.06184
	0.7				1.05177
0.8	0.3	0.2	0.01	1.5	1.00351
		0.4			0.97573
		0.6			0.94845
0.8	0.3	0.2	0.02	1.5	0.95618
			0.03		0.92579
			0.04		0.90693
0.8	0.3	0.2	0.02	1.5	0.91854
				2.5	0.89576
				3.5	0.85454

Table. 3. Impact of different physical factors on $Sh_x Re_x^{-0.5} = -\Phi'(0)$

Sc	N_b	N_t	Pr	$Sh_x Re_x^{-0.5}$
0.4	0.3	0.2	1.5	0.80086
0.8				0.80661
1.0				0.81244
0.4	0.3	0.2	1.5	0.82553
	0.5			0.80046
	0.7			0.77852
0.4	0.3	0.2	1.5	0.77113
		0.4		0.79778
		0.6		0.79868
0.4	0.3	0.2	1.5	0.775714
			2.5	0.765212
			3.5	0.748865

Since the bioconvection Lewis and Peclet numbers are inversely proportional to the diffusion of microorganism, so the growth in L_b, P_e decline the values of $\xi(\eta)$ due to which density rate of motile is augmented as portrayed in Table 4. The rate of motile density has also augmented numerically with upsurge in inclination angle as shown in Table 4.

Tables 5 and 6 present a comparative analysis for HAM solutions and numerical solutions with a fine agreement amongst all the results.

Table. 4. Impact of different physical factors on $Nn_x Re_x^{-0.5} = -\xi'(0)$

Pr	P_e	L_b	Ω	$Nn_x Re_x^{-0.5}$
1.5	0.5	0.5	0.2	1.02064
2.5				0.99062
3.5				0.97574
1.5	0.5	0.5		1.04039
	1.0			1.13978
	1.5			1.24021
1.5	0.5	0.5		1.25417
		0.6		1.28226
		0.7		1.31057
1.5	0.5	0.5	0.2	1.29451
			0.4	1.32664
			0.6	1.35877

Table. 5. Comparison between HAM and numerical solutions for $f'(\eta)$

η	**HAM solution**	**Numerical soltuion**	**Absolute Error**
0.0	0.700000	0.700000	0.000000
0.5	0.175994	0.175896	0.000098
1.0	0.176936	0.176795	0.000141
1.5	0.167316	0.167108	0.000213
2.0	0.154481	0.154174	0.000307
2.5	0.145614	0.145002	0.000512
3.0	0.145748	0.145054	0.000694
3.5	0.126644	0.125711	0.000933
4.0	0.128527	0.127304	0.001223
4.5	0.129903	0.128029	0.001874
5.0	0.118101	0.115265	0.002836
5.5	0.116428	0.114293	0.003135
6.0	0.116578	0.112905	0.003673

Table. 6. Comparison between HAM and numerical solutions are shown for $\theta(\eta)$

η	**HAM solution**	**Numerical soltuion**	**Absolute Error**
0.0	0.100000	0.100000	0.000000
0.5	0.114961	0.114065	0.000896
1.0	0.115984	0.115007	0.000977
1.5	0.117473	0.116212	0.001261
2.0	0.106243	0.104501	0.001742
2.5	0.1083249	0.1080761	0.002488
3.0	0.986563	0.983459	0.002794
3.5	0.984502	0.981007	0.003495
4.0	0.869275	0.865401	0.003874
4.5	0.869547	0.865294	0.004253
5.0	0.797502	0.792115	0.005387
5.5	0.744753	0.738842	0.005911
6.0	0.707409	0.701016	0.006393

4.7. HAM Convergence

The solution's convergence of current model has ensured through $\hbar$-curves like $\hbar_f$, $\hbar_\theta$, $\hbar_\phi$ and $\hbar_\chi$ using HAM approach as depicted in Figures 17(a-d) where the approximation has used up to 15 order. The region of convergence has also depicted in the relevant graphs for all the characteristics

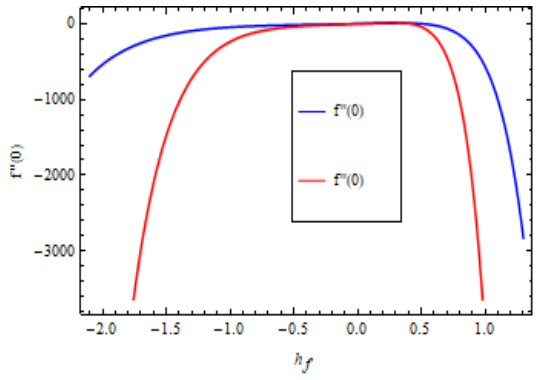

(a)

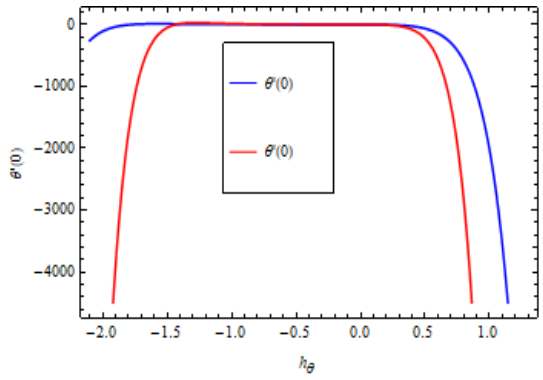

(b)

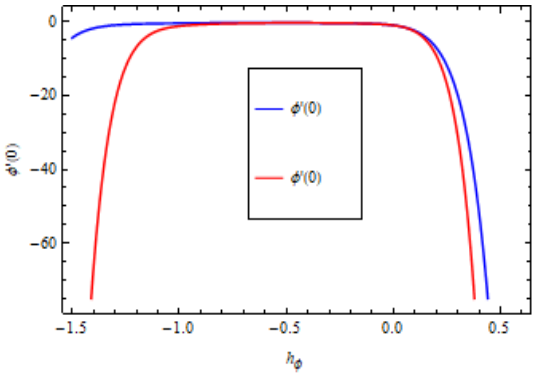

(c)

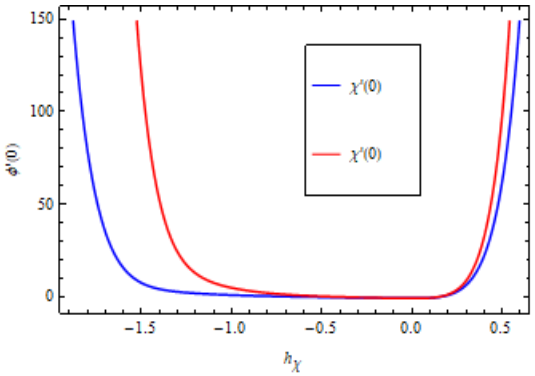

(d)

Fig. 17. Convergence of HAM solution for variations in $\hbar_f$, $\hbar_\theta$, $\hbar_\phi$ & $\hbar_\chi$

5. Conclusions

This work investigates nonlinear mixed convective hybrid nanofluid flow on a porous and inclined stretching plat. The flow is influenced by porous behavior of the plate and the presence of the microorganisms. Main emphasis is given to analyze the influence of thermal and mass Grashof numbers for their nonlinear nature upon the flow system. The equations that administered the flow system are converted to dimension-free notations by suitable variables. After extensive insight into the work, the following points have been noticed.

- An upsurge in the values of inertial factor results dominancy in the inertial forces due to which maximum constraints is experienced by the fluid particles at the surface of inclined plate that declines the motion of fluid.
- With higher values of porosity factor, the ability to flow in the porous medium is reduced and retards fluid velocity.
- For higher values of magnetic factor a declining force against motion of fluid is produced that acts as a reducing agent for fluid motion.
- The number of nanoparticles augments the density of fluid at the inclined plate. When the dense behavior of fluid upsurges, then, as a consequence, the fluid particles observe more constraint to flow.
- With growth in Brownian factor, the haphazard motion with in the fluid upsurge due to more collision amongst the particles that converts the kinetic energy to heat energy, as a result of which thermal flow upsurges.
- When the values of thermophoresis factor get higher, then the temperature gradient is also getting higher that maximizes the width of temperature layer at the boundaries.
- With higher values of Prandtl number, the spread of temperature is restricted, due to which the width of the thermal boundary is reduced and causes an augmentation in temperature characteristics.
- Upsurge in Eckert number has caused a hike in thermal energy sharing in the flow of fluid and has upsurge the flow regime that augmented the thermal flow profiles.
- When the values of the Brownian factor upsurge, then thermal characteristics augment that support skin friction, due to which less mass transportation occurs and ultimately declines the concentration profiles.
- For growth in thermophoresis factor plenty of nanoparticles move away from the hot surface of inclined plate due to which the volume fraction distribution upsurge and augments the concentration of fluid.
- With growth in Sc the particles of fluid at the surface of inclined plate defuse at minimum level as a result of which lesser mass transportation of fluid occurs.
- Since both of Peclet and bioconvection Lewis numbers are inversely proportional to diffusion of microorganism (D_m), so with growth in these factors less diffusion occurs in microorganism that justifies the decline in density number of microorganism.
- For upsurge in the values of inclination angle fewer microbes are shifted to the upper surface of the fluid due to which the diffusion of microorganism affected adversely.

- The influence of many emerging factors on skin friction, Nusselt, Sherwood and density numbers have been described numerically in tabular form.
- The study depicts that in case of $Nb, Nt, Ec \in [1, 4]$ the heat transfer rate varies from 1.8057 to 2.1332 in case of growth in Brownian factor, it varies from 1.8057 to 2.1968 in case of variation in thermophoresis factor while it varies from 1.8057 to 2.3177 in case of growth in Eckert number. Maximum growth in thermal flow rate has noticed in case of escalation in Eckert number.
- In future, the impacts of variable porous space will be incorported in current model and its stability ananlysis will be carried out in parallel.
- HAM solution has also compared with a numerical solution, with a small error noticed amongst all results.

Funding Statement

This research did not receive any specific grant from funding agencies in the public, commercial, or not-for-profit sectors.

Conflicts of Interest

The author declares that there is no conflict of interest regarding the publication of this article.

Data Availability Statement:

The data that support the findings of this study are available upon reasonable request from the authors.

References

[1] Muhammad, R., Khan, M. I., Jameel, M., & Khan, N. B., 2020. Fully developed Darcy-Forchheimer mixed convective flow over a curved surface with activation energy and entropy generation. Computer Methods and Programs in Biomedicine, 188, 105298.

[2] Waini, I., Ishak, A., & Pop, I., 2020. Mixed convection flow over an exponentially stretching/shrinking vertical surface in a hybrid nanofluid. Alexandria Engineering Journal, 59(3), 1881-1891.

[3] Safdar, R., Jawad, M., Hussain, S., Imran, M., Akgül, A., & Jamshed, W., 2022. Thermal radiative mixed convection flow of MHD Maxwell nanofluid: Implementation of buongiorno's model. Chinese Journal of Physics, 77, 1465-1478.

[4] Nabwey, H. A., EL-Kabeir, S. M. M., Rashad, A. M., & Abdou, M. M. M., 2022. Gyrotactic microorganisms mixed convection flow of nanofluid over a vertically surfaced saturated porous media. Alexandria Engineering Journal, 61(3), 1804-1822.

[5] Wahid, N. S., Arifin, N. M., Khashi'ie, N. S., Pop, I., Bachok, N., & Hafidzuddin, M. E. H., 2022. MHD mixed convection flow of a hybrid nanofluid past a permeable vertical flat plate with thermal radiation effect. Alexandria Engineering Journal, 61(4), 3323-3333.

[6] Ali, B., Liu, S., Jubair, S., Khalifa, H. A. E. W., & Abd El-Rahman, M., 2023. Exploring the impact of Hall and ion slip effects on mixed convective flow of Casson fluid Model: A stochastic investigation through non-Fourier double diffusion theories using ANNs techniques. Thermal Science and Engineering Progress, 46, 102237.

[7] Choi, S. U., & Eastman, J. A., 1995. Enhancing thermal conductivity of fluids with nanoparticles (No. ANL/MSD/CP-84938; CONF-951135-29). Argonne National Lab.(ANL), Argonne, IL (United States).

[8] Sharma, R. P., Badak, K., Mishra, S. R., & Ahmed, S., 2023. Behavior of hybrid nanostructure and dust particles in fluid motion with thermal radiation and memory effects. The European Physical Journal Plus, 138(2), 159.

[9] Chu, Y. M., Bashir, S., Ramzan, M., & Malik, M. Y., 2022. Model-based comparative study of magnetohydrodynamics unsteady hybrid nanofluid flow between two infinite parallel plates with particle shape effects. Mathematical Methods in the Applied Sciences.

[10] Khan, A., Hassan, B., Ashraf, E. E., & Shah, S. Y. A., 2022. Thermally dissipative micropolar hybrid nanofluid flow over a spinning needle influenced by Hall current and gyrotactic microorganisms. Heat Transfer, 51(1), 1170-1192.

[11] Eid, M. R., & Nafe, M. A., 2022. Thermal conductivity variation and heat generation effects on magneto-hybrid nanofluid flow in a porous medium with slip condition. Waves in Random and Complex Media, 32(3), 1103-1127.

[12] Ojjela, O., 2022. Numerical investigation of heat transport in Alumina–Silica hybrid nanofluid flow with modeling and simulation. Mathematics and Computers in Simulation, 193, 100-122.

[13] Ali, B., Jubair, S., Aluraikan, A., Abd El-Rahman, M., Eldin, S. M., & Khalifa, H. A. E. W., 2023. Numerical investigation of heat source induced thermal slip effect on trihybrid nanofluid flow over a stretching surface. Results in Engineering, 20, 101536.

[14] Gumber, P., Yaseen, M., Rawat, S. K., & Kumar, M., 2022. Heat transfer in micropolar hybrid nanofluid flow past a vertical plate in the presence of thermal radiation and suction/injection effects. Partial Differential Equations in Applied Mathematics, 5, 100240.

[15] Ali, B., Jubair, S., Fathima, D., Akhter, A., Rafique, K., & Mahmood, Z., 2023. MHD flow of nanofluid over moving slender needle with nanoparticles aggregation and viscous dissipation effects. Science Progress, 106(2), 00368504231176151.

[16] Ali, B., AlBaidani, M. M., Jubair, S., Ganie, A. H., & Abdelmohsen, S. A., 2023. Computational framework of hydrodynamic stagnation point flow of nanomaterials with natural convection configured by a heated stretching sheet. ZAMM-Journal of Applied Mathematics and Mechanics/Zeitschrift für Angewandte Mathematik und Mechanik, e202200542.

[17] Ali, B., Mishra, N. K., Rafique, K., Jubair, S., Mahmood, Z., & Eldin, S. M., 2023. Mixed convective flow of hybrid nanofluid over a heated stretching disk with zero-mass flux using the modified Buongiorno model. Alexandria Engineering Journal, 72, 83-96.

[18] Elattar, S., Helmi, M. M., Elkotb, M. A., El-Shorbagy, M. A., Abdelrahman, A., Bilal, M., & Ali, A., 2022. Computational assessment of hybrid nanofluid flow with the influence of hall current and chemical reaction over a slender stretching surface. Alexandria Engineering Journal, 61(12), 10319-10331.

[19] Sabu, A. S., Mackolil, J., Mahanthesh, B., & Mathew, A., 2022. Nanoparticle aggregation kinematics on the quadratic convective magnetohydrodynamic flow of nanomaterial past an inclined flat plate with sensitivity analysis. Proceedings of the Institution of Mechanical Engineers, Part E: Journal of Process Mechanical Engineering, 236(3), 1056-1066.

[20] Kodi, R., & Mopuri, O., 2022. Unsteady MHD oscillatory Casson fluid flow past an inclined vertical porous plate in the presence of chemical reaction with heat absorption and Soret effects. Heat Transfer, 51(1), 733-752.

[21] Osman, H. I., Omar, N. F. M., Vieru, D., & Ismail, Z., 2022. A Study of MHD Free Convection Flow Past an Infinite Inclined Plate. Journal of Advanced Research in Fluid Mechanics and Thermal Sciences, 92(1), pp. 18-27.

[22] Jha, B. K., & Samaila, G., 2022. The Combined Impact of Thermal Radiation and Thermophoresis on Buoyancy-Driven Flow Near an Inclined Porous Plate. Journal of Heat Transfer, 144(10).

[23] Sheri, S. R., Peesu, M., & Mamidi Narsimha, R., 2022. Hall current, chemical reaction, and radiation results on transient magnetohydrodynamic flow past an inclined plate: FEM. Heat Transfer, 51(2), pp. 1876-1899.

[24] Hazarika, S., Ahmed, S., & Yao, S. W., 2023. Investigation of Cu–water nano-fluid of natural convection hydro-magnetic heat transport in a Darcian porous regime with diffusion-thermo. Applied Nanoscience, 13(1), 283-293.

[25] Ali, L., Liu, X., Ali, B., Mujeed, S., Abdal, S., & Khan, S. A., 2020. Analysis of magnetic properties of nano-particles due to a magnetic dipole in micropolar fluid flow over a stretching sheet. Coatings, 10(2), 170.

[26] Sarada, K., Gowda, R. J. P., Sarris, I. E., Kumar, R. N., & Prasannakumara, B. C., 2021. Effect of magnetohydrodynamics on heat transfer behaviour of a non-Newtonian fluid flow over a stretching sheet under local thermal non-equilibrium condition. Fluids, 6(8), p. 264.

[27] Reza-E-Rabbi, S., Ahmmed, S. F., Arifuzzaman, S. M., Sarkar, T., & Khan, M. S., 2020. Computational modelling of multiphase fluid flow behaviour over a stretching sheet in the presence of nanoparticles. Engineering Science and Technology, an International Journal, 23(3), pp. 605-617.

[28] Warke, A. S., Ramesh, K., Mebarek-Oudina, F., & Abidi, A., 2022. Numerical investigation of the stagnation point flow of radiative magnetomicropolar liquid past a heated porous stretching sheet. Journal of Thermal Analysis and Calorimetry, 147(12), pp. 6901-6912.

[29] Guedri, K., Khan, A., Gul, T., Mukhtar, S., Alghamdi, W., Yassen, M. F., & Tag Eldin, E., 2022. Thermally Dissipative Flow and Entropy Analysis for Electromagnetic Trihybrid Nanofluid Flow Past a Stretching Surface. ACS omega.

[30] Shah, S. A. A., Ahammad, N. A., Din, E. M. T. E., Gamaoun, F., Awan, A. U., & Ali, B., 2022. Bio-convection effects on prandtl hybrid nanofluid flow with chemical reaction and motile microorganism over a stretching sheet. Nanomaterials, 12(13), 2174.

[31] Hazarika, S., Ahmed, S., & Chamkha, A. J., 2021. Investigation of nanoparticles Cu, Ag and Fe3O4 on thermophoresis and viscous dissipation of MHD nanofluid over a stretching sheet in a porous regime: a numerical modeling. Mathematics and Computers in Simulation, 182, 819-837.

[32] Waqas, H., Imran, M., Muhammad, T., Sait, S. M., & Ellahi, R., 2020. On bio-convection thermal radiation in Darcy–Forchheimer flow of nanofluid with gyrotactic motile microorganism under Wu's slip over stretching cylinder/plate. International Journal of Numerical Methods for Heat & Fluid Flow.

[33] Yusuf, T. A., Mabood, F., Prasannakumara, B. C., & Sarris, I. E., 2021. Magneto-bioconvection flow of Williamson nanofluid over an inclined plate with gyrotactic microorganisms and entropy generation. Fluids, 6(3), 109.

[34] Khan, A., Saeed, A., Tassaddiq, A., Gul, T., Mukhtar, S., Kumam, P., & Kumam, W., 2021. Bio-convective micropolar nanofluid flow over thin moving needle subject to Arrhenius activation energy, viscous dissipation and binary chemical reaction. Case Studies in Thermal Engineering, 25, 100989.

[35] Bhatti, M. M., Arain, M. B., Zeeshan, A., Ellahi, R., & Doranehgard, M. H., 2022. Swimming of Gyrotactic Microorganism in MHD Williamson nanofluid flow between rotating circular plates embedded in porous medium: Application of thermal energy storage. Journal of Energy Storage, 45, 103511.

[36] Das, B., & Ahmed, S., 2023. Numerical modeling of bioconvection and heat transfer analysis of Prandtl nanofluid in an inclined stretching sheet: A finite difference scheme. Numerical Heat Transfer, Part A: Applications, 1-21.

[37] Shah, S. A., Mouldi, A., & Sene, N., 2022. Nonlinear Convective SiO2 and TiO2 Hybrid Nanofluid Flow over an Inclined Stretched Surface. Journal of Nanomaterials, 2022.

[38] Gul, T., Mukhtar, S., Alghamdi, W., Ali, I., Saeed, A., & Kumam, P., 2022. Entropy and Bejan Number Influence on the Liquid Film Flow of Viscoelastic Hybrid Nanofluids in a Porous Space in Terms of Heat Transfer. ACS omega.

[39] Yazdi, M. E., Moradi, A., & Dinarvand, S., 2014. MHD mixed convection stagnation-point flow over a stretching vertical plate in porous medium filled with a nanofluid in the presence of thermal radiation. Arabian journal for science and engineering, 39, 2251-2261.

[40] Liao, S. J., 1999. Explicit totally analytic approximate solution for Blasius viscous flow problems. International Journal of Non-Linear Mechanics, 34, 759-778.

[41] Liao, S. J., 2010. An optimal homotopy analysis approach for strongly nonlinear differential equations. Communications in Nonlinear Science and Numerical Simulation, 15(8), pp.2003-2016.